

Self-Supervised Audio-Visual Representation Learning with Relaxed Cross-Modal Temporal Synchronicity

Pritam Sarkar ^{1,2} Ali Etemad ¹

¹Queen’s University, Canada ²Vector Institute

{pritam.sarkar, ali.etemad}@queensu.ca

<https://pritamqu.github.io/CrissCross>

Abstract

We present **CrissCross**, a self-supervised framework for learning audio-visual representations. A novel notion is introduced in our framework whereby in addition to learning the intra-modal and standard ‘synchronous’ cross-modal relations, CrissCross also learns ‘asynchronous’ cross-modal relationships. We show that by relaxing the temporal synchronicity between the audio and visual modalities, the network learns strong time-invariant representations. Our experiments show that strong augmentations for both audio and visual modalities with relaxation of cross-modal temporal synchronicity optimize performance. To pretrain our proposed framework, we use 3 different datasets with varying sizes, Kinetics-Sound, Kinetics-400, and AudioSet. The learned representations are evaluated on a number of downstream tasks namely action recognition, sound classification, and retrieval. CrissCross shows state-of-the-art performances on action recognition (UCF101 and HMDB51) and sound classification (ESC50). The codes and pretrained models will be made publicly available .

1. Introduction

In recent years, self-supervised learning has shown great promise in learning strong representations without human-annotated labels [9, 11, 12], minimizing the gap between self-supervised and fully-supervised pretraining. There are a number of benefits to such methods. Firstly, they reduce the time and resources required for expensive human-annotations and allow researchers to directly use large uncurred datasets for learning meaningful representations. Moreover, the models trained in a self-supervised fashion learn more abstract representations, which can be useful in solving a variety of downstream tasks without needing to train the models from scratch.

Given the abundance of videos, their spatio-temporal information-rich nature, and the fact that in most cases they contain both audio and visual streams, self-supervised approaches are strong alternatives to fully-supervised methods

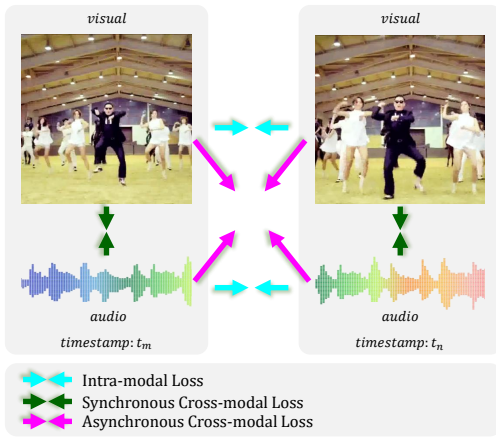


Figure 1. We present an overview of our method. CrissCross learns effective audio-visual multi-modal representations not only by considering intra-modal relationships, but also by learning synchronous cross-modal as well as *asynchronous* cross-modal relations. The sample frames are obtained from Kinetics-400 [22].

for video representation learning. Moreover, the high dimensionality and multi-modal nature of videos makes them difficult to annotate, further motivates the use of self-supervision.

A thorough review of the literature on self-supervised audio-visual representation learning reveals the following open problems. (i) Data augmentation is proven to induce invariance toward learning strong representations [11, 62], yet little attention has been paid to investigate different augmentation strategies in multi-modal self-supervised frameworks. (ii) Given that many existing works on video-based self-supervised learning take direct inspiration from image-based methods [2, 26, 47, 50], they do not take full advantage of temporal information available in video data. For instance, methods based on contrastive frameworks [11, 32, 37, 39, 40, 44], distillation [12, 17], quantization [3, 9, 10], or information maximization [68], require two augmented views of a given sample to be fed to a shared backbone, followed by optimizing the underlying cost function. As also identified in a recent work [48], we observe that many video-based methods [2, 26, 47] perform the necessary augmentations on temporally identical views. (iii) Lastly, existing solutions try to

learn audio-visual representations by maintaining a tight temporal synchronicity between the two modalities [2, 3, 5, 26]. Yet, the impact of learning temporally asynchronous cross-modal relationships in the context of self-supervised learning has not been explored. This notion deserves deeper exploration as learning such temporally asynchronous cross-modal relationships may in fact result in additional invariance and distinctiveness in the learned representations.

In this study, in an attempt to address the above-mentioned issues, we present **CrissCross** (a simple illustration is presented in Figure 1), a novel framework to learn robust time-invariant representations from videos. First, we leverage the ‘time’ information available in videos and explore efficient ways of sampling audio-visual segments from given source video clips. Our empirical studies show that with properly composed temporal sampling and the right amount of spatial augmentations, the model learns strong representations useful for a variety of downstream tasks. Second, we introduce a novel concept to learn cross-modal representations through relaxing time-synchronicity between audio and visual segments, which we refer to as ‘asynchronous cross-modal’ optimization. We use 3 datasets of different sizes: Kinetics-Sound [4], Kinetics-400 [22], and AudioSet [16], to pretrain CrissCross. We evaluate CrissCross on different downstream tasks, namely action recognition, sound classification, and retrieval. We use 2 popular benchmarks UCF101 [57] and HMDB51 [27] to perform action recognition and retrieval, while ESC50 [46] is used for sound classification.

Contributions. The key contributions of this work are as follows: **(1)** We present a novel framework for multi-modal self-supervised learning by relaxing the audio-visual temporal synchronicity to learn effective time-invariant representations. Our method is a simple, yet effective solution to learn robust multi-modal representations for downstream tasks. **(2)** We perform an in-depth study to explore the proposed framework and its major concepts. Additionally we extensively investigate a wide range of audio-visual augmentation techniques towards learning strong audio-visual representations in a multi-modal setup. **(3)** Comparing the performance of the proposed framework to prior works, CrissCross achieves state-of-the-arts on UCF101 [57], HMDB [27], and ESC50 [46] when pretrained on Kinetics-400 [22]. Moreover, CrissCross outperforms fully-supervised pretraining when trained on the same small-scale dataset like Kinetics-Sound [4] and set new state-of-the-arts. To the best of our knowledge, CrissCross is the first to show that self-supervised pretraining outperforms full supervision on action recognition on such a small-scale dataset. Additionally, when CrissCross is trained with a very large-scale dataset AudioSet [16], it achieves better or competitive performances with respect to the current state-of-the-arts. We hope our proposed self-supervised method can motivate researchers

to further explore the notion of *asynchronous* multi-modal representation learning.

2. Related Work

2.1. Self-supervised Learning

Self-supervised learning aims to learn generalized representations of data without any human annotated labels through properly designed pseudo tasks (also known as pretext tasks). Self-supervised learning has recently drawn significant attention in different fields of deep learning such as image [9–12, 17, 37, 50], video [2, 3, 5, 36, 39, 40, 44], and wearable data [53–55] analysis among others.

In self-supervised learning, the main focus of interest lies in designing novel pseudo-tasks to learn useful representations. We briefly mention some of the popular categories in the context of self-supervised video representation learning, namely, *i*) context-based, *ii*) generation-based, *iii*) clustering-based, and *iv*) contrastive learning-based. Various pretext tasks have been proposed in the literature exploring the spatio-temporal context of video frames, for example, temporal order prediction [28], puzzle solving [1, 24, 38], rotation prediction [21], and others. Generation-based video feature learning methods refer to the process of learning feature representations through video generation [52, 61, 63], video colorization [59], and frame or clip prediction [7, 15, 29, 33, 49], among a few others. Clustering-based approaches [3, 5] rely on self-labeling where data is fed to the network and the extracted feature embeddings are clustered using a classical clustering algorithm such as k-means, followed by using the cluster assignments as the pseudo-labels for training the neural network. The key concept of contrastive learning [10, 12, 17, 37, 40, 44] is that in the embedding space, ‘positive’ samples should be similar to each other, and ‘negative’ samples should have discriminative properties. Using this concept, several prior works [32, 39, 40, 44] have attempted to learn representations by minimizing the distance between positive pairs and maximizing the distance between negative pairs.

2.2. Audio-Visual Representation Learning

Typically in multi-modal self-supervised learning, multiple networks are jointly trained on the same pretext tasks towards maximizing the mutual information between multiple data streams [3, 23, 26, 40, 56, 64, 66]. Following, we briefly discuss some of the prior works [3, 26, 32, 40] on audio-visual multi-modal representation learning. A multi-modal self-supervised task introduced in AVTS [26], leveraging the natural synergy between audio-visual data. The network is trained to distinguish whether the given audio and visual sequences are ‘in sync’ or ‘out of sync’. The authors propose a two-stream network, where one stream receives audio as input and the other network is fed with the visual data.

Next, audio and visual embeddings are fused at the end of the convolution layers, and the joint representations are used to minimize the contrastive loss. In XDC [3], the authors introduce a framework to learn cross-modal representations through a self-labelling process. In XDC, cluster assignments obtained from the audio-visual representations are used as pseudo-labels to train the backbones. Specifically, the pseudo-labels computed from audio embeddings are used to train the visual backbone, while the pseudo-labels computed using visual embeddings are used to train the audio network. A self-supervised learning framework based on contrastive learning is proposed in AVID [40], to learn audio-visual representations from video. AVID performs instance discrimination as the pretext task. AVID [40] redefines the notion of positive and negative pairs based on their similarity and dissimilarity in the feature space, followed by optimizing a noise contrastive estimator loss to learn multi-modal representations. This is different from AVTS [26], where audio-visual segments originated from the same samples are considered as positive pairs, and segments originated from different samples are considered as negative pairs.

Distinctions to our work. We acknowledge that earlier works [26, 32, 40] show great promise in learning strong multimodal representations, however, we identify some limitations, which we attempt to address in our study. Most of the earlier works based on contrastive learning try to find negative pairs and positive pairs through a complex process. We also notice that over the time, the definition of ‘positive’ and ‘negative’ pairs have been changing. For instance, we find distinct differences in such definitions amongst some earlier works [26, 39, 40]. In this study, our goal is to propose a simple yet effective solution towards learning multi-modal representations. Additionally, we would like highlight that earlier works [3, 5, 32, 40] use a massive distributed GPU setup (40-64 GPUs), which is a significant bottleneck when computing resources are limited. In this study, we effectively train our method on 4-8 GPUs. Lastly, as discussed earlier, we hypothesize that to learn effective time-invariant features, the synchronicity between audio and visual segments could be relaxed. Interestingly, it may appear that our approach is in contrast to some prior works that suggest synchronization [26, 48] is helpful in learning strong multi-modal representations. Nonetheless, our framework exploits both synchronous and asynchronous cross-modal relationships in an attempt to learn both time-dependant and time-invariant representations.

3. Method

In this section we present the core concepts of our proposed framework. First, we briefly discuss the uni-modal concepts that our model is build on, which are adopted from an earlier work, SimSiam [12]. Next, we introduce the multi-modal concepts of our framework to jointly learn audio-

visual representations in a self-supervised setup.

3.1. Uni-modal Learning

To separately learn visual and audio representations, we follow the setup proposed in [12], which we briefly mention here for the sake of completeness. Let’s, assume an encoder f , where f is composed of a convolutional backbone followed by an MLP projection head, and an MLP prediction head h . Two augmented views of a sample x are created as x_1 and x_2 . Accordingly, the objective is to minimize the symmetrized loss:

$$\mathcal{L}_{x_1, x_2} = \frac{1}{2}\mathcal{D}(p_1, \mathbb{S}(z_2)) + \frac{1}{2}\mathcal{D}(p_2, \mathbb{S}(z_1)), \quad (1)$$

where \mathcal{D} denotes the negative cosine similarity, and output vectors p_1 and z_2 are computed as $h(f(x_1))$ and $f(x_2)$ respectively. Similarly, p_2 and z_1 are computed as $h(f(x_2))$ and $f(x_1)$ respectively. Further, we apply stop-grad on the latent vector z_1 and z_2 , which is denoted by \mathbb{S} . We extend this concept to learn visual and audio representations as discussed below.

To learn visual representations from videos, we use a visual encoder f_v and a predictor head h_v . We generate two augmented views of a sample v as v_1 and v_2 , where v_1 belongs to timestamp t_1 , and v_2 belongs to timestamp t_2 . Finally, we optimize the loss \mathcal{L}_{v_1, v_2} using Equation 1. We present this concept in Figure 2(A). Similarly we generate two augmented views of an audio sample a as a_1 and a_2 , where a_1 and a_2 belong to timestamps t_1 and t_2 respectively. We use a_1 and a_2 to optimize \mathcal{L}_{a_1, a_2} (following Equation 1) using an audio encoder f_a and a predictor head h_a to learn audio representations. A pictorial representation of this method is depicted in Figure 2(B).

3.2. Multi-modal Learning

Here, we discuss the multi-modal learning components of our proposed framework. We present different ways to learn multi-modal representations, namely Intra-modal, Synchronous Cross-modal, Asynchronous Cross-modal, and finally, CrissCross, which blends all three previous methods. We explain each of these concepts below.

Intra-modal Representations. To learn multi-modal representations, our first approach is a joint representation learning method where we train the visual and audio networks with a common objective function \mathcal{L}_{intra} . Here, \mathcal{L}_{intra} is calculated as $(\mathcal{L}_{v_1, v_2} + \mathcal{L}_{a_1, a_2})/2$, where \mathcal{L}_{v_1, v_2} and \mathcal{L}_{a_1, a_2} are uni-modal losses for visual and audio learning as discussed earlier.

Synchronous Cross-modal Representations. To learn cross-modal audio-visual representations, we calculate the distance between the two different modalities, particularly by calculating \mathcal{L}_{a_1, v_1} corresponding to a_1 , v_1 , and \mathcal{L}_{a_2, v_2} , corresponding to a_2 , v_2 . Finally, we optimize the syn-

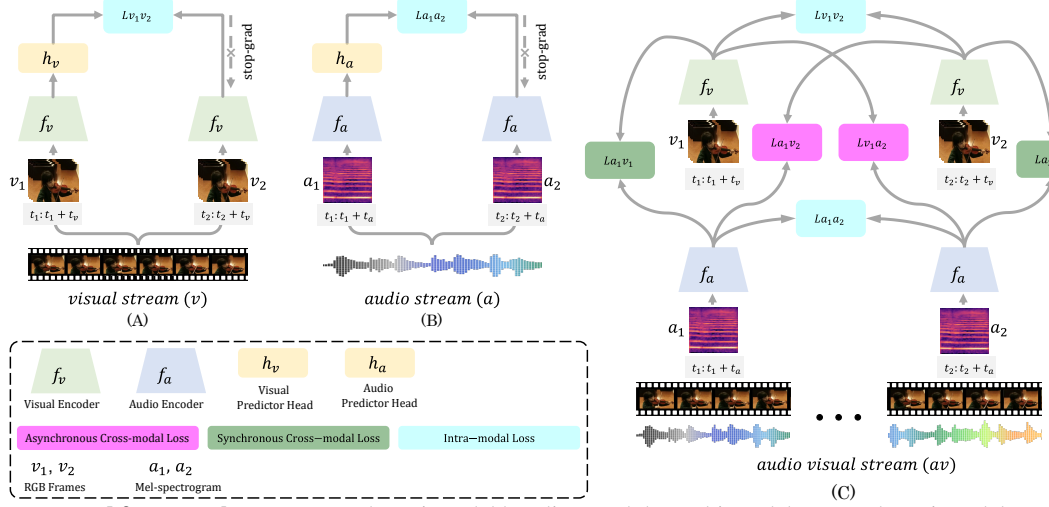


Figure 2. **Our proposed framework.** We present the uni-modal baselines and the multi-modal setup. The uni-modal setups (Visual-only and Audio-only) are presented in (A) and (B) respectively. The multi-modal framework, CrissCross, is presented in (C). In case of uni-modal setups, we show the predictor heads, as well as the stop-grad to elaborate on the frameworks. However, in case of CrissCross, we skip those components for the sake of simplicity.

chronous cross-modal loss \mathcal{L}_{sync} , which is calculated as $(\mathcal{L}_{a_1, v_1} + \mathcal{L}_{a_2, v_2})/2$.

Asynchronous Cross-modal Representations. Next, we introduce an *asynchronous* (or cross-time) cross-modal loss to learn local time-invariant representations. Here, we attempt to optimize *asynchronous* cross-modal representations by calculating \mathcal{L}_{a_1, v_2} to minimize the distance between feature vectors corresponding to a_1 and v_2 . Similarly, we calculate \mathcal{L}_{a_2, v_1} to minimize the distance between feature vectors corresponding to a_2 and v_1 . Finally, we calculate the asynchronous cross-modal loss \mathcal{L}_{async} as $(\mathcal{L}_{a_1, v_2} + \mathcal{L}_{a_2, v_1})/2$.

CrissCross. Our proposed multi-modal representation learning method is named CrissCross. In this setup, we combine the objective functions of Intra-modal, Synchronous Cross-modal, and Asynchronous Cross-modal learning. Accordingly, we define the final objective function $\mathcal{L}_{CrissCross}$ as $(\mathcal{L}_{intra} + \mathcal{L}_{sync} + \mathcal{L}_{async})/3$, which gives:

$$\mathcal{L}_{CrissCross} = \frac{1}{6}(\mathcal{L}_{a_1, a_2} + \mathcal{L}_{v_1, v_2} + \mathcal{L}_{a_1, v_1} + \mathcal{L}_{a_2, v_2} + \mathcal{L}_{a_1, v_2} + \mathcal{L}_{a_2, v_1}). \quad (2)$$

We present the proposed CrissCross framework in Figure 2(C) and its pseudocode in Section S1.

3.3. Relaxing Time Synchronicity

Audio and visual modalities from the same source clip generally maintain a very strong correlation, which makes them suitable for multi-modal representation learning as one modality can be used as a supervisory signal for the other in a self-supervised setup. However, our intuition behind CrissCross is that these cross-modal temporal correlations do not necessarily need to follow a strict frame-wise coupling. Instead, we hypothesize that relaxing cross-modal

temporal synchronicity to some extent can help in learning more generalized representations.

To facilitate this idea within CrissCross, we present 5 different temporal sampling methods to create the augmented views of a source clip. These 5 **temporal sampling methods** are designed to explore varying amounts of **temporal synchronicity** when learning cross-modal relationships. (i) *Same-timestamp*: where both the audio and visual segments are sampled from the exact same time window (denoted as *none* in terms of temporal relaxation). (ii) *Overlapped*: where the two views of the audio-visual segments share 50% overlap amongst them (denoted as *mild* relaxation). (iii) *Adjacent*: where adjacent frame sequences and audio segments are sampled (denoted as *medium* relaxation). (iv) *Far-apart*: in which we sample one view from the first half of the source clip, while the other view is sampled from the second half of the source clip (denoted as *extreme* relaxation). (v) *Random*: where the two audio-visual segments are sampled in a temporally random manner (denoted as *mixed* relaxation). It should be noted that the concept of relaxing cross-modal time synchronicity doesn't apply to the uni-modal setups.

4. Experiment

The details of the experiment setup and the findings of our thorough empirical studies for investigating the major concepts of our proposed framework are presented here.

4.1. Experiment Setup

Datasets. We use 3 datasets of different sizes for pretraining purposes, namely, Kinetics-Sound [4], Kinetics400 [22], and AudioSet [16]. Following the standard practices of prior works [2, 3, 5, 26, 39, 40], we evaluate our self-supervised methods on two types of downstream tasks, (i) action recog-

nition using UCF101 [57] and HMDB51 [27], and (ii) sound classification using ESC50 [46]. We provide additional details for all the datasets in Section S3.

Architectures. Following the standard practice among prior works [3, 5, 39, 40, 44] we use R(2+1)D [60] and ResNet [20] as the visual and audio backbones. We use a slightly modified version [40] of R(2+1)D-18 [60] as the backbone for visual feature extraction. To extract the audio features, we use ResNet-18 [20]. The projector and predictor heads of the self-supervised framework are composed of MLPs. The details of all of the architectures are presented in Section S6.

Pretraining Details. To train the network in a self-supervised fashion with audio-visual inputs, we downsample the visual streams to 16 frames per second, and feed 0.5-second frame sequences to the visual encoder. We resize the spatial resolution to 112^2 , so the final input dimension to the visual encoder becomes $3 \times 8 \times 112^2$, where 3 represents the 3 channels of RGB. Next, we downsample the audio signals to 16kHz, and segment them into 2-second segments. Next, we transform the segmented raw audio waveforms to mel-spectrograms using 80 mel filters, we set the hop size as 10 milliseconds, and FFT window length as 1024. Finally, we feed spectrograms of shape 80×200 to the audio encoder. We use Adam [25] optimizer with a cosine learning rate scheduler [30] to pretrain the encoders and use a fixed learning rate to train the predictors. We provide additional details of the hyperparameters in Section S4.

4.2. Empirical Study

Here we present the empirical study performed to investigate the major concepts of our proposed framework. During the empirical study all of the models are trained using Kinetics-Sound [4] for 100 epochs, unless stated otherwise. We perform transfer learning to evaluate visual and audio representations. Linear evaluation is performed using a one-vs-all SVM classifier (linear kernel) on the fixed features to quickly evaluate our models on downstream tasks. We prefer one-vs-all SVM over training an FC layer to limit parameter tuning at this point. Moreover, to limit memory overhead, we use 0.5 seconds (8 frames) of visual input and 2 seconds of audio input to extract the fixed features. The details of the linear evaluation protocol is mentioned in Section S5. We use UCF101 to evaluate visual representations on action recognition, and ESC50 to evaluate audio representation on sound classification. All of our empirical studies are evaluated using split-1 of both the datasets.

4.2.1 Ablation Study

We present the ablation results in Table 1 to show the improvement made by optimizing intra-modal, synchronous cross-modal, and asynchronous cross-modal losses. First, we train the framework in uni-modal setups, denoted as \mathcal{L}_{v_1, v_2} and \mathcal{L}_{a_1, a_2} . We report the top-1 accuracy of UCF101 and

Table 1. **Ablation study.** We present the results of CrissCross and its uni-modal and multi-modal ablation variants.

Method	UCF101	ESC50
(a) \mathcal{L}_{v_1, v_2}	69.1	–
(b) \mathcal{L}_{a_1, a_2}	–	62.0
(c) \mathcal{L}_{intra}	69.7	71.8
(d) \mathcal{L}_{sync}	70.1	75.8
(e) \mathcal{L}_{async}	69.1	74.8
(f) $\mathcal{L}_{sync} + \mathcal{L}_{intra}$	73.8	78.0
(g) $\mathcal{L}_{async} + \mathcal{L}_{intra}$	72.4	75.3
(h) $\mathcal{L}_{async} + \mathcal{L}_{sync}$	69.1	74.8
(i) $\mathcal{L}_{CrissCross}$	74.8	79.0

ESC50 as 69.1% and 62.0% respectively. Next, we train the network in a multi-modal setup, where we find that \mathcal{L}_{sync} outperforms the other multi-modal variants with single-term losses (Table 1(c) to 1(e)) as well as uni-modal baselines (Table 1(a) and 1(b)). Further study shows that combining different multi-modal losses (Table 1(f) to 1(i)) improve the model performance. Specifically, we notice that $\mathcal{L}_{CrissCross}$ outperforms \mathcal{L}_{sync} by 4.7% and 3.2% on action recognition and sound classification, respectively.

We further investigate the benefits of $\mathcal{L}_{CrissCross}$ versus the top 2 ablation competitors ($\mathcal{L}_{sync} + \mathcal{L}_{intra}$ and $\mathcal{L}_{async} + \mathcal{L}_{intra}$) on the large and diverse Kinetics-400 [22]. We observe that $\mathcal{L}_{CrissCross}$ outperforms these variants by 4.1% and 3.5% in action recognition and sound classification, respectively, showing the significance of asynchronous cross-modal optimization in a multi-modal setup. Our intuition is that as Kinetics-Sound consists of a few hand-picked classes that are prominently manifested in both audio and visual modalities, the performance gain of CrissCross is less prominent. However, Kinetics-400 is considerably larger in scale and is comprised of highly diverse action classes. It therefore benefits more from the more generalized representations learned by asynchronous cross-modal optimization. Additional results for Kinetics-400 can be found in Section S7.

4.2.2 Understanding Relaxed Time-synchronicity

In this subsection we study how different amounts of temporal relaxation in cross-modal synchronicity impacts CrissCross. To do so, we exploit 5 different temporal sampling methods as discussed earlier in Section 3. We further aim to identify the best temporal sampling method in a uni-modal setup. We train Visual-only, Audio-only, and CrissCross frameworks using different temporal sampling methods. The results presented in Table 2 show that the *overlapped* sampling method works the best overall for both the uni-modal setups. The *same* temporal sampling method shows poor performance on the visual-only model. However, it performs as good as the *overlapped* sampling method on the audio-only model. Interestingly, the *far-apart* sampling shows the worst performance amongst other methods on the Audio-only model, whereas, the Visual-only model works reasonably well with the *far-apart* sampling method. Next, we

Table 2. **Temporal sampling.** Exploring temporal sampling methods for multi-modal and uni-modal representation learning.

Temp. Sampling (Temp. Relaxation)	Uni-modal		CrissCross	
	UCF101	ESC50	UCF101	ESC50
Same (None)	55.6	62.0	73.2	77.0
Overlapped (Mild)	68.3	62.0	73.9	79.0
Adjacent (Medium)	68.1	58.8	71.5	77.8
Random (Random)	65.1	60.3	72.5	77.8
Far-apart (Extreme)	63.8	58.3	72.8	78.5

Table 3. **Augmentations.** Exploring audio-visual augmentations.

Video Augs.	UCF101	Audio Augs.	ESC50
	UCF101		ESC50
Uni	MSC–HF–CJ	62.3	VJ
	MSC–HF–CJ–GS	68.1	VJ–M
	MSC–HF–CJ–GS–C	68.3	VJ–M–TW
	MSC–HF–CJ–GS–GB	68.7	VJ–M–RC
	MSC–HF–CJ–GS–GB–C	69.1	
Video Augs. + Audio Augs.		UCF101	ESC50
Multi	MSC–HF–CJ–GS–C + VJ–M–RC	73.9	79.0
	MSC–HF–CJ–GS–GB + VJ–M–RC	73.5	79.0
	MSC–HF–CJ–GS–GB–C + VJ–M–RC	74.8	79.0

test these 5 temporal sampling methods on CrissCross and present the results in Table 2. Interestingly, we notice that the *same* and *far-apart* methods, which work poorly in the uni-modal setups, perform reasonably well in a multi-modal setup. We believe, the improvement of performance here is because of the strong supervision received from the other modality. Nonetheless, we find that the *overlapped* temporal sampling method (*mild* temporal relaxation) performs relatively better, outperforming the other approaches.

4.2.3 Exploring Audio-Visual Augmentations

We perform an in-depth study to explore the impact of different audio and visual augmentations.

Visual Augmentations. We explore a wide range of visual augmentations. As a starting point, we adopt the basic spatial augmentations used in [40], which consists of Multi-Scale Crop (MSC), Horizontal Flip (HF), and Color Jitter (CJ). Additionally, we explore other augmentations, namely Gray Scale (GS), Gaussian Blur (GB) [11], and Cutout (C) [14], which show great performance in image-based self-supervised learning [11, 62]. We explore almost all the possible combinations of different visual augmentations in a uni-modal setup and present the results in Table 3. The results show that strong augmentations improve the top-1 accuracy by 6.8% in comparison to basic augmentations used in [40]. We mention the augmentation parameters and implementation details in Section S2.

Temporal Consistency of Spatial Augmentations. While investigating different spatial augmentations, we are also interested to know if the spatial augmentations should be consistent at the frame level or whether they should be random (i.e., vary among consecutive frames within a sequence). We refer to these concepts as *temporally consistent* or *temporally random*. We perform an experiment where we apply

Table 4. **Predictor learning rate.** A comparative study of different predictor learning rates with respect to the base learning rate.

	UCF101		ESC50	
	Base LR	10×Base LR	Base LR	10×Base LR
\mathcal{L}_{a_1, a_2}	-	-	60.3	62.0
\mathcal{L}_{v_1, v_2}	66.0	69.1	-	-
$\mathcal{L}_{CrissCross}$	59.0	74.8	62.3	79.0

MSC–HF–CJ–GS randomly at the frame level, and compare the results to applying the same augmentations consistently across all the frames of a sequence. Our results show that maintaining temporal consistency in spatial augmentations across consecutive frames is beneficial, which is in line with the findings in [47]. Specifically, *Temporally random* augmentations, results in top-1 accuracy of 53.69%, whereas, the same augmentations applied in a *temporally consistent* manner results in 68.09%.

Audio Augmentations. Similar to visual augmentations, we thoroughly investigate a variety of audio augmentations. Our audio augmentations include, Volume Jitter (VJ), Time and Frequency Masking (Mask) [42], Random Crop (RC) [41], and Time Warping (TW) [42]. We also explore almost all the possible combinations of these augmentations, and present the results in Table 3. Our findings show that time-frequency masking and random crop improve the top-1 accuracy by 17.25% compared to the base variant. We also notice that time warping doesn't improve the performance and is also quite computationally expensive. Hence, going forward we do not use time warping during pretraining. We present the augmentation parameters and additional implementation details in Section S2.

Audio-Visual Augmentations. We conduct further experiments on a few combinations of augmentations in a *multi-modal* setup. We pick the top performing augmentations obtained from the uni-modal variants and apply them concurrently. The results are presented in Table 3 where we find that the results are consistent with the uni-modal setups, as the combination of MSC–HF–CJ–GS–GB–C and VJ–M–RC performs the best in comparison to the other combinations.

4.2.4 Exploring Design Choices

Predictor. Our empirical study shows that the predictor head plays an important role to effectively train the audio and visual encoders to learn good representations. The predictor architecture is similar to [12]. For the sake of completeness, we provide the details of the predictor head in Section S6. We explore (i) different learning rates, and (ii) using a common vs. a separate predictor in the multi-modal setup. It should be noted that none of the variants cause a collapse, even though we notice considerable differences in performance. We present the findings in the following paragraphs.

Similar to [12], we use a constant learning rate for the predictors. However, unlike [12], where the predictor learning rate is the same as the base learning rate of the encoder, we

Table 5. **Design choice.** Exploring design choices for the predictor and projector heads.

	Predictor		Projector	
	Common	Separate	2 Layers	3 Layers
UCF101	73.6	74.8	72.4	74.8
ESC50	75.3	79.0	75.0	79.0

find that a higher predictor learning rate helps the network to learn better representations in both uni-modal and multi-modal setups. In case of CrissCross, setting the predictor learning rate to be the same as the base learning rate results in unstable training, and the loss curve shows oscillating behavior. We empirically find that setting the predictor learning rate to 10 times the base learning rate, works well. We present the results in Table 4.

Next, we evaluate whether the framework can be trained in a multi-modal setup with a common predictor head instead of separate predictor heads (default setup). In simple terms, one predictor head would work towards identity mapping for both audio and video feature vectors. To test this, l2-normalized feature vectors $f_v(v)$ and $f_a(a)$ are fed to the predictor, which are then used in a usual manner to optimize the cost function. The results are presented in Table 5. We observe that though such a setup works somewhat well, having separate predictors is beneficial for achieving a more stable training and learning better representations.

Projector. We present a comparative study of projector heads with 2 layers vs. 3 layers. We notice that 2.4%, and 4% improvements in top-1 accuracies when using 3 layers instead of 2 on action recognition and sound classification respectively (please refer to Table 5). Note that we use 3 fully-connected layers as the default setup for the projectors. The details of the architecture are presented in Section S6.

5. Comparison to the State-of-the-Arts

We compare the proposed CrissCross framework against the state-of-the-arts methods. We validate visual representations on action recognition, and audio representations on sound classification. We present the details in the following.

5.1. Action Recognition

Full-Finetuning. In line with [3, 5, 32, 40, 44, 48], we benchmark CrissCross using UCF101 [57] and HMDB51 [27] on action recognition. We briefly mention the experimental setup for downstream evaluation here and redirect readers to Section S5 for additional information. We use the pretrained 18-layer R(2+1)D [60] as the video backbone, and fully finetune it on action recognition. We use the Kinetics-Sound [4], Kinetics-400 [22], and AudioSet [16] for pretraining. For a fair comparison to earlier works, we adopt 2 setups for finetuning, once with 8 frames, and the other with 32 frames. In both these setups, we use a spatial resolution of 224^2 . We tune the model using the split-1 of both datasets and report

Table 6. **State-of-the-art comparison on action recognition.** Top-1 accuracy averaged over all the splits on UCF101 and HMDB51 are presented. We group the results based on the pre-training dataset. Additionally, we present the architecture details and finetuning input size of the respective methods.

Method	Backbone	Finetune Input Size	UCF101	HMDB51
Pretraining Dataset: Kinetics-Sound (22K)				
Fully Supervised [32]	3D-ResNet18	32×224^2	86.9	53.1
CM-ACC [32]	3D-ResNet18	32×224^2	77.2	40.6
CrissCross	R(2+1)D-18	8×224^2	84.0	51.2
	R(2+1)D-18	32×224^2	88.3	60.5
Pretraining Dataset: Kinetics-400 (240K)				
Fully Supervised [44]	R(2+1)D-18	32×224^2	95.0	74.0
AVTS [26]	MC3-18	25×224^2	84.1	52.5
SeLaVi [5]	R(2+1)D-18	32×112^2	83.1	47.1
XD-C [3]	R(2+1)D-18	8×224^2	74.2	39.0
	R(2+1)D-18	32×224^2	86.8	52.6
AVID [40]	R(2+1)D-18	8×224^2	83.7	49.5
	R(2+1)D-18	32×224^2	87.5	60.8
GDT [44]	R(2+1)D-18	32×224^2	89.3	60.0
Robust-xID [39]	R(2+1)D-18	8×224^2	81.9	49.5
	R(2+1)D-18	32×224^2	85.6	55.0
CrissCross	R(2+1)D-18	8×224^2	86.9	54.3
	R(2+1)D-18	32×224^2	91.5	64.7
Pretraining Dataset: AudioSet (1.8M)				
Fully Supervised [48]	R(2+1)D-18	32×224^2	96.8	75.9
AVTS [26]	MC3-18	25×224^2	87.7	57.3
XD-C [3]	R(2+1)D-18	8×224^2	84.9	48.8
	R(2+1)D-18	32×224^2	91.2	61.0
AVID [40]	R(2+1)D-18	8×224^2	88.6	57.6
	R(2+1)D-18	32×224^2	91.5	64.7
GDT [44]	R(2+1)D-18	32×224^2	92.5	66.1
MMV [2]	R(2+1)D-18	32×224^2	91.5	70.1
BraVe [48]	R(2+1)D-18	32×224^2	94.1	71.1
CM-ACC [32]	R(2+1)D-18	32×224^2	93.5	67.2
CrissCross	R(2+1)D-18	8×224^2	89.4	58.3
	R(2+1)D-18	32×224^2	92.4	66.8

the top-1 accuracy averaged over all the splits.

The comparison of CrissCross with recent prior works is presented in Table 6. To save computation time and resources, the fully-supervised baselines compared to CrissCross, are taken directly from prior works [3, 36, 44, 48] and have not been implemented by ourselves. When pretrained with Kinetics-400, CrissCross achieves state-of-the-arts on UCF101 and HMDB51 in both the fine-tuning setups. CrissCross outperforms current state-of-the-arts AVID [40] on UCF101 and HMDB51 by 3.2% and 4.8%, respectively, when fine-tuned with 8 frame inputs. Additionally, while fine-tuned with 32 frames, CrissCross outperforms current state-of-the-arts GDT [44] and AVID [40] by 2.2% and 3.9% on UCF101 and HMDB51 respectively. CrissCross shows significant improvements compared to CM-ACC [32] on UCF101 (77.2 vs. 88.3) and HMDB51 (40.6 vs. 60.5) when pretrained using a small-scale dataset Kinetics-Sound [4].

Table 7. **State-of-the-art comparison on action recognition retrieval performance.** We present the accuracy of video retrieval on UCF and HMDB datasets for different numbers of nearest neighbors, using the video backbone pretrained on Kinetics400.

Method	UCF			HMDB		
	R@1	R@5	R@20	R@1	R@5	R@20
Clip Order [66]	14.1	30.3	51.1	7.6	22.9	48.8
VCP [31]	18.6	33.6	53.5	7.6	24.4	53.6
VSP [13]	24.6	41.9	76.9	10.3	26.6	54.6
CoCLR [19]	55.9	70.8	82.5	26.1	45.8	69.7
SeLaVi [5]	52.0	68.6	84.5	24.8	47.6	75.5
GDT [44]	57.4	73.4	88.1	25.4	51.4	75.0
Robust-xID [39]	60.9	79.4	90.8	30.8	55.8	79.7
CrissCross	63.8	78.7	89.9	26.4	50.5	77.7

Additionally, CrissCross outperforms fully-supervised baselines by 1.4% and 7.4% on UCF101 and HMDB51 respectively when both the fully-supervised and self-supervised methods are pretrained on Kinetics-Sound [4]. To the best of our knowledge, this is the first time that self-supervision outperforms fully-supervised pretraining on action recognition using the same small-scale dataset, showing that our method even performs well on limited pretraining data. Finally, CrissCross outperforms the current state-of-the-art, AVID [40], when pretrained on AudioSet and fine-tuned with 8-frame inputs, on both UCF101 and HMDB51. Next, when fine-tuned with 32-frame inputs, CrissCross achieves competitive results amongst the leading methods. It should be noted that prior works which show slightly better performance compared to CrissCross are trained with much longer visual input segments. For example, BraVe [48] uses 2 augmented views of 32 and 128 frames, whereas CrissCross takes only 8 frames as input for both views. Please see Section S7 for an extended list of comparisons.

Retrieval. In addition to full finetuning, we also compare the performance of CrissCross in an unsupervised setup. Following prior works [5, 39, 44], we perform a retrieval experiment. We use the split-1 of both UCF101 [57] and HMDB51 [27] and present the comparison with prior works in Table 7. We observe that CrissCross outperforms the current state-of-the-arts on UCF101, while achieving competitive results for HMDB51. We present additional details for the retrieval experiment setup in Section S5.

5.2. Sound Classification

To evaluate audio representations learned by CrissCross, we use a popular benchmark ESC50 [46] to perform sound classification. We find large variability of experimental setups in the literature for evaluating audio representations. For example, different backbones, different input lengths, different datasets, and different evaluation protocols (linear evaluation, full-finetuning) have been used, making it impractical to compare to all the prior works. Following [2, 26, 39, 40, 48], we perform linear classification using one-vs-all SVM. For

Table 8. **State-of-the-art comparison on sound classification.** Top-1 accuracy averaged over all the splits on ESC50 is presented. Additionally, we present the linear evaluation input size and the architecture details of the respective methods.

Method	Backbone	Input	ESC50	
			Kinetics-400	AudioSet
AVTS [26]	VGG-8	2 sec.	76.7	80.6
XDC [3]	ResNet-18	2 sec.	78.0	84.8
AVID [40]	ConvNet-9	2 sec.	79.1	89.1
GDT [44]	ResNet-9	2 sec.	-	88.5
MMV [2]	ResNet-50	5 sec.	-	85.6
BraVe [48]	ResNet-50	5 sec.	-	90.4
CrissCross	ResNet-18	2 sec.	81.5	86.7
	ResNet-18	5 sec.	86.8	90.5

the sake of fair comparison with a wide range of prior works, we perform linear evaluation using 2 and 5-second inputs. We redirect readers to Section S5 for additional details of the evaluation protocols and Section S7 for an extended list of comparisons. As presented in Table 8, when pretrained on Kinetics-400 and evaluated with 2-second inputs, CrissCross outperforms the current state-of-the-art AVID [40] by 2.4%. Additionally, when pretrained on AudioSet and evaluated with 5-second inputs, CrissCross marginally outperforms the current state-of-the-art, BraVe [48].

6. Summary

We propose a novel self-supervised framework to learn audio-visual representations by considering intra-modal, as well as, synchronous and *asynchronous* cross-modal relationships. We conduct a thorough study investigating the major concepts of our framework. Our findings show that properly composed strong augmentations and relaxation of cross-modal temporal synchronicity is beneficial for learning effective audio-visual representations. These representations can then be used for a variety of downstream tasks including action recognition, sound classification, and retrieval.

Limitations. The notion of asynchronous cross-modal optimization has not been explored beyond audio-visual modalities. For example, our model can be expanded to consider more than 2 modalities (e.g., audio, visual, and text), which we are yet to study. Additionally, we notice a considerable performance gap between full-supervision and self-supervision when both methods are pretrained with the same large-scale dataset (Kinetics-400 or AudioSet), showing room for further improvement.

Broader Impact. Better self-supervised audio-visual learning can be used for detection of harmful content on the Internet. Additionally, such methods can be used to develop better multimedia systems and tools. Lastly, the notion that relaxed cross-modal temporal synchronicity is useful, can challenge our existing/standard approaches in learning multi-modal representations and result in new directions of inquiry. The authors don't foresee any major negative impacts.

Acknowledgment

We are grateful to Bank of Montreal and Mitacs for funding this research. We are thankful to Vector Institute and SciNet HPC Consortium for helping with the computation resources.

References

- [1] Unaiza Ahsan, Rishi Madhok, and Irfan Essa. Video jigsaw: Unsupervised learning of spatiotemporal context for video action recognition. In *WACV*, pages 179–189, 2019. [2](#)
- [2] Jean-Baptiste Alayrac, Adria Recasens, Rosalia Schneider, Relja Arandjelovic, Jason Ramapuram, Jeffrey De Fauw, Lucas Smaira, Sander Dieleman, and Andrew Zisserman. Self-supervised multimodal versatile networks. *NeurIPS*, 2(6):7, 2020. [1, 2, 4, 7, 8, 13, 14, 16](#)
- [3] Humam Alwassel, Dhruv Mahajan, Bruno Korbar, Lorenzo Torresani, Bernard Ghanem, and Du Tran. Self-supervised learning by cross-modal audio-video clustering. *NeruIPS*, 33, 2020. [1, 2, 3, 4, 5, 7, 8, 13, 14, 16](#)
- [4] Relja Arandjelovic and Andrew Zisserman. Look, listen and learn. In *ICCV*, pages 609–617, 2017. [2, 4, 5, 7, 8, 12, 13, 16](#)
- [5] Yuki M. Asano, Mandela Patrick, Christian Rupprecht, and Andrea Vedaldi. Labelling unlabelled videos from scratch with multi-modal self-supervision. In *NeurIPS*, 2020. [2, 3, 4, 5, 7, 8, 13, 14, 16](#)
- [6] Yusuf Aytar, Carl Vondrick, and Antonio Torralba. Soundnet: Learning sound representations from unlabeled video. *NeurIPS*, 29:892–900, 2016. [16](#)
- [7] Mohammad Babaeizadeh, Chelsea Finn, Dumitru Erhan, Roy H Campbell, and Sergey Levine. Stochastic variational video prediction. In *ICLR*, 2018. [2](#)
- [8] Sagie Benaim, Ariel Ephrat, Oran Lang, Inbar Mosseri, William T Freeman, Michael Rubinstein, Michal Irani, and Tali Dekel. Speednet: Learning the speediness in videos. In *CVPR*, pages 9922–9931, 2020. [16](#)
- [9] Mathilde Caron, Piotr Bojanowski, Armand Joulin, and Matthijs Douze. Deep clustering for unsupervised learning of visual features. In *ECCV*, pages 132–149, 2018. [1, 2](#)
- [10] Mathilde Caron, Ishan Misra, Julien Mairal, Priya Goyal, Piotr Bojanowski, and Armand Joulin. Unsupervised learning of visual features by contrasting cluster assignments. In *NeurIPS*, 2020. [1, 2](#)
- [11] Ting Chen, Simon Kornblith, Mohammad Norouzi, and Geoffrey Hinton. A simple framework for contrastive learning of visual representations. In *ICML*, pages 1597–1607, 2020. [1, 2, 6, 12](#)
- [12] Xinlei Chen and Kaiming He. Exploring simple siamese representation learning. In *CVPR*, pages 15750–15758, 2021. [1, 2, 3, 6, 13, 15](#)
- [13] Hyeon Cho, Taehoon Kim, Hyung Jin Chang, and Wonjun Hwang. Self-supervised spatio-temporal representation learning using variable playback speed prediction. *arXiv preprint arXiv:2003.02692*, 2020. [8](#)
- [14] Terrance DeVries and Graham W Taylor. Improved regularization of convolutional neural networks with cutout. *arXiv preprint arXiv:1708.04552*, 2017. [6](#)
- [15] Chelsea Finn, Ian Goodfellow, and Sergey Levine. Unsupervised learning for physical interaction through video prediction. *NeurIPS*, 29:64–72, 2016. [2](#)
- [16] Jort F Gemmeke, Daniel PW Ellis, Dylan Freedman, Aren Jansen, Wade Lawrence, R Channing Moore, Manoj Plakal, and Marvin Ritter. Audio set: An ontology and human-labeled dataset for audio events. In *ICASSP*, pages 776–780, 2017. [2, 4, 7, 12, 13](#)
- [17] Jean-Bastien Grill, Florian Strub, Florent Altché, Corentin Tallec, Pierre Richemond, Elena Buchatskaya, Carl Doersch, Bernardo Pires, Zhaohan Guo, Mohammad Azar, et al. Bootstrap your own latent: A new approach to self-supervised learning. In *NeurIPS*, 2020. [1, 2](#)
- [18] Tengda Han, Weidi Xie, and Andrew Zisserman. Video representation learning by dense predictive coding. In *CVPRW*, pages 0–0, 2019. [16](#)
- [19] Tengda Han, Weidi Xie, and Andrew Zisserman. Self-supervised co-training for video representation learning. In *NeurIPS*, 2020. [8](#)
- [20] Kaiming He, Xiangyu Zhang, Shaoqing Ren, and Jian Sun. Deep residual learning for image recognition. In *CVPR*, pages 770–778, 2016. [5, 15](#)
- [21] Longlong Jing, Xiaodong Yang, Jingen Liu, and Yingli Tian. Self-supervised spatiotemporal feature learning via video rotation prediction. *arXiv preprint arXiv:1811.11387*, 2018. [2, 16](#)
- [22] Will Kay, Joao Carreira, Karen Simonyan, Brian Zhang, Chloe Hillier, Sudheendra Vijayanarasimhan, Fabio Viola, Tim Green, Trevor Back, Paul Natsev, et al. The kinetics human action video dataset. *arXiv preprint arXiv:1705.06950*, 2017. [1, 2, 4, 5, 7, 12, 15, 16](#)
- [23] Aparna Khare, Srinivas Parthasarathy, and Shiva Sundaram. Self-supervised learning with cross-modal transformers for emotion recognition. In *SLT*, pages 381–388, 2021. [2](#)
- [24] Dahun Kim, Donghyeon Cho, and In So Kweon. Self-supervised video representation learning with space-time cubic puzzles. In *AAAI*, volume 33, pages 8545–8552, 2019. [2, 16](#)
- [25] Diederik P Kingma and Jimmy Ba. Adam: A method for stochastic optimization. In *ICLR*, 2015. [5, 13](#)
- [26] Bruno Korbar, Du Tran, and Lorenzo Torresani. Cooperative learning of audio and video models from self-supervised synchronization. In *NeruIPS*, pages 7774–7785, 2018. [1, 2, 3, 4, 7, 8, 13, 16](#)
- [27] Hildegarde Kuehne, Hueihan Jhuang, Estíbaliz Garrote, Tomaso Poggio, and Thomas Serre. Hmdb: a large video database for human motion recognition. In *ICCV*, pages 2556–2563, 2011. [2, 5, 7, 8, 13, 14](#)
- [28] Hsin-Ying Lee, Jia-Bin Huang, Maneesh Singh, and Ming-Hsuan Yang. Unsupervised representation learning by sorting sequences. In *CVPR*, 2017. [2](#)
- [29] Xiaodan Liang, Lisa Lee, Wei Dai, and Eric P Xing. Dual motion gan for future-flow embedded video prediction. In *ICCV*, pages 1744–1752, 2017. [2](#)
- [30] Ilya Loshchilov and Frank Hutter. Sgdr: Stochastic gradient descent with warm restarts. In *ICLR*, 2017. [5](#)

[31] Dezhao Luo, Chang Liu, Yu Zhou, Dongbao Yang, Can Ma, Qixiang Ye, and Weiping Wang. Video cloze procedure for self-supervised spatio-temporal learning. In *AAAI*, 2020. 8

[32] Shuang Ma, Zhaoyang Zeng, Daniel McDuff, and Yale Song. Active contrastive learning of audio-visual video representations. In *ICLR*, 2020. 1, 2, 3, 7, 16

[33] Michael Mathieu, Camille Couprie, and Yann LeCun. Deep multi-scale video prediction beyond mean square error. In *ICLR*, 2016. 2

[34] Brian McFee, Colin Raffel, Dawen Liang, Daniel PW Ellis, Matt McVicar, Eric Battenberg, and Oriol Nieto. librosa: Audio and music signal analysis in python. In *Python in Science Conference*, volume 8, pages 18–25, 2015. 12

[35] Paulius Micikevicius, Sharan Narang, Jonah Alben, Gregory Diamos, Erich Elsen, David Garcia, Boris Ginsburg, Michael Houston, Oleksii Kuchaiev, Ganesh Venkatesh, et al. Mixed precision training. In *ICLR*, 2018. 13

[36] Shaobo Min, Qi Dai, Hongtao Xie, Chuang Gan, Yongdong Zhang, and Jingdong Wang. Cross-modal attention consistency for video-audio unsupervised learning. *arXiv preprint arXiv:2106.06939*, 2021. 2, 7

[37] Ishan Misra and Laurens van der Maaten. Self-supervised learning of pretext-invariant representations. In *CVPR*, pages 6707–6717, 2020. 1, 2

[38] Ishan Misra, C Lawrence Zitnick, and Martial Hebert. Shuffle and learn: unsupervised learning using temporal order verification. In *ECCV*, pages 527–544, 2016. 2

[39] Pedro Morgado, Ishan Misra, and Nuno Vasconcelos. Robust audio-visual instance discrimination. In *CVPR*, pages 12934–12945, 2021. 1, 2, 3, 4, 5, 7, 8, 13, 14, 16

[40] Pedro Morgado, Nuno Vasconcelos, and Ishan Misra. Audio-visual instance discrimination with cross-modal agreement. In *CVPR*, pages 12475–12486, 2021. 1, 2, 3, 4, 5, 6, 7, 8, 12, 13, 14, 15, 16

[41] Daisuke Niizumi, Daiki Takeuchi, Yasunori Ohishi, Noboru Harada, and Kunio Kashino. Byol for audio: Self-supervised learning for general-purpose audio representation. *arXiv preprint arXiv:2103.06695*, 2021. 6, 12

[42] Daniel S Park, William Chan, Yu Zhang, Chung-Cheng Chiu, Barret Zoph, Ekin D Cubuk, and Quoc V Le. Specaugment: A simple data augmentation method for automatic speech recognition. *arXiv preprint arXiv:1904.08779*, 2019. 6, 12

[43] Adam Paszke, Sam Gross, Francisco Massa, Adam Lerer, James Bradbury, Gregory Chanan, Trevor Killeen, Zeming Lin, Natalia Gimelshein, Luca Antiga, et al. Pytorch: An imperative style, high-performance deep learning library. *NeurIPS*, 32:8026–8037, 2019. 12, 13

[44] Mandela Patrick, Yuki M. Asano, Polina Kuznetsova, Ruth Fong, João F. Henriques, Geoffrey Zweig, and Andrea Vedaldi. Multi-modal self-supervision from generalized data transformations. *ICCV*, 2021. 1, 2, 5, 7, 8, 14, 16

[45] Karol J Piczak. Environmental sound classification with convolutional neural networks. In *MLSP*, pages 1–6, 2015. 16

[46] Karol J. Piczak. ESC: Dataset for Environmental Sound Classification. In *ACM Conference on Multimedia*, pages 1015–1018, 2015. 2, 5, 8, 13, 16

[47] Rui Qian, Tianjian Meng, Boqing Gong, Ming-Hsuan Yang, Huisheng Wang, Serge Belongie, and Yin Cui. Spatiotemporal contrastive video representation learning. In *CVPR*, pages 6964–6974, 2021. 1, 6

[48] Adrià Recasens, Pauline Luc, Jean-Baptiste Alayrac, Luyu Wang, Florian Strub, Corentin Tallec, Mateusz Malinowski, Viorica Patraucean, Florent Altché, Michal Valko, et al. Broaden your views for self-supervised video learning. *arXiv preprint arXiv:2103.16559*, 2021. 1, 3, 7, 8, 13, 14, 16

[49] Fitsum A Reda, Guilin Liu, Kevin J Shih, Robert Kirby, Jon Barker, David Tarjan, Andrew Tao, and Bryan Catanzaro. Sdc-net: Video prediction using spatially-displaced convolution. In *ECCV*, pages 718–733, 2018. 2

[50] Shuvendu Roy and Ali Etemad. Self-supervised contrastive learning of multi-view facial expressions. In *ICMI*, pages 253–257, 2021. 1, 2

[51] Hardik B Sailor, Dharmesh M Agrawal, and Hemant A Patil. Unsupervised filterbank learning using convolutional restricted boltzmann machine for environmental sound classification. In *Interspeech*, volume 8, page 9, 2017. 16

[52] Masaki Saito, Eiichi Matsumoto, and Shunta Saito. Temporal generative adversarial nets with singular value clipping. In *ICCV*, pages 2830–2839, 2017. 2

[53] Pritam Sarkar and Ali Etemad. Self-supervised ecg representation learning for emotion recognition. *IEEE Transactions on Affective Computing*, 2020. 2

[54] Pritam Sarkar and Ali Etemad. Self-supervised learning for ecg-based emotion recognition. In *ICASSP*, pages 3217–3221, 2020. 2

[55] Pritam Sarkar, Silvia Lobmaier, Bibiana Fabre, Gabriela Berg, Alexander Mueller, Martin G Frasch, Marta C Antonelli, and Ali Etemad. Detection of maternal and fetal stress from ecg with self-supervised representation learning. *arXiv e-prints*, pages arXiv–2011, 2020. 2

[56] Shamane Siriwardhana, Tharindu Kaluarachchi, Mark Billinghurst, and Suranga Nanayakkara. Multimodal emotion recognition with transformer-based self supervised feature fusion. *IEEE Access*, 8:176274–176285, 2020. 2

[57] Khurram Soomro, Amir Roshan Zamir, and Mubarak Shah. Ucf101: A dataset of 101 human actions classes from videos in the wild. *arXiv preprint arXiv:1212.0402*, 2012. 2, 5, 7, 8, 13, 14

[58] Chen Sun, Fabien Baradel, Kevin Murphy, and Cordelia Schmid. Learning video representations using contrastive bidirectional transformer. *arXiv preprint arXiv:1906.05743*, 2019. 16

[59] Du Tran, Lubomir Bourdev, Rob Fergus, Lorenzo Torresani, and Manohar Paluri. Deep end2end voxel2voxel prediction. In *CVPRW*, pages 17–24, 2016. 2

[60] Du Tran, Heng Wang, Lorenzo Torresani, Jamie Ray, Yann LeCun, and Manohar Paluri. A closer look at spatiotemporal convolutions for action recognition. In *CVPR*, pages 6450–6459, 2018. 5, 7, 15

[61] Sergey Tulyakov, Ming-Yu Liu, Xiaodong Yang, and Jan Kautz. MoCoGAN: Decomposing motion and content for video generation. In *CVPR*, pages 1526–1535, 2018. 2

[62] Wouter Van Gansbeke, Simon Vandenhende, Stamatis Georgoulis, Marc Proesmans, and Luc Van Gool. Scan: Learning to classify images without labels. In *ECCV*, pages 268–285, 2020. [1](#), [6](#)

[63] Carl Vondrick, Hamed Pirsiavash, and Antonio Torralba. Generating videos with scene dynamics. *NeurIPS*, 29:613–621, 2016. [2](#)

[64] Jiangliu Wang, Jianbo Jiao, Linchao Bao, Shengfeng He, Wei Liu, and Yun-Hui Liu. Self-supervised video representation learning by uncovering spatio-temporal statistics. *PAMI*, 2021. [2](#)

[65] Jiangliu Wang, Jianbo Jiao, Linchao Bao, Shengfeng He, Yunhui Liu, and Wei Liu. Self-supervised spatio-temporal representation learning for videos by predicting motion and appearance statistics. In *CVPR*, pages 4006–4015, 2019. [16](#)

[66] Dejing Xu, Jun Xiao, Zhou Zhao, Jian Shao, Di Xie, and Yueling Zhuang. Self-supervised spatiotemporal learning via video clip order prediction. In *CVPR*, pages 10334–10343, 2019. [2](#), [8](#), [14](#), [16](#)

[67] Yang You, Igor Gitman, and Boris Ginsburg. Large batch training of convolutional networks. *arXiv preprint arXiv:1708.03888*, 2017. [13](#)

[68] Jure Zbontar, Li Jing, Ishan Misra, Yann LeCun, and Stéphane Deny. Barlow twins: Self-supervised learning via redundancy reduction. *arXiv preprint arXiv:2103.03230*, 2021. [1](#)

Change Log

- V1: Initial release.
- V2: Minor modifications in the text.

Supplementary Material

In this supplementary material we provide additional details of our experimental setup and results as follows:

- Section **S1**: Pseudocode;
- Section **S2**: Details of data augmentations;
- Section **S3**: Details of all the datasets;
- Section **S4**: Hyperparameters and training details;
- Section **S5**: Downstream evaluation protocols;
- Section **S6**: Architecture details;
- Section **S7**: Additional results and analysis.

S1. Algorithms

We present the pseudocode of our proposed CrissCross framework in Algorithm 1. Please note this pseudocode is written in a Pytorch-like format.

Algorithm 1 CrissCross pseudocode (PyTorch-like)

```

class CrissCross(nn.Module):
    def __init__(fv, fa, hv, ha):
        super().__init__()
        """Initialize CrissCross Module
        Args:
            fv: video encoder (backbone+projection mlp)
            fa: audio encoder (backbone+projection mlp)
            hv: video predictor (prediction mlp)
            ha: audio predictor (prediction mlp)
        Returns:
            CrissCross Module
        """

    def forward(v1, v2, a1, a2):
        """Forward function CrissCross Module
        Args:
            v1, v2: minibatch of augmented video samples
            a1, a2: minibatch of augmented audio samples
        Returns:
            L_CrissCross: total loss
        """

        # video
        zv1, zv2 = fv(v1), fv(v2) # video embeddings
        pv1, pv2 = hv(zv1), hv(zv2) # predictor output

        # audio
        za1, za2 = fa(a1), fa(a2) # audio embeddings
        pa1, pa2 = ha(za1), ha(za2) # predictor output

        # loss calculation
        # D: loss function

        # asynchronous cross-modal loss
        Lv1a2 = D(pv1, za2)/2 + D(pa2, zv1)/2 # v1-a2
        La1v2 = D(pa1, zv2)/2 + D(pv2, za1)/2 # a1-v2
        L_async = (Lv1a2 + La1v2)/2

        # synchronous cross-modal loss
        Lv1a1 = D(pv1, za1)/2 + D(pa1, zv1)/2 # v1-a1
        Lv2a2 = D(pv2, za2)/2 + D(pa2, zv2)/2 # v2-a2
        L_sync = (Lv1a1 + Lv2a2)/2

        # intra-modal loss
        Lv1v2 = D(pv1, zv2)/2 + D(pv2, zv1)/2 # v1-v2
        La1a2 = D(pa1, za2)/2 + D(pa2, za1)/2 # a1-a2
        L_intra = (Lv1v2 + La1a2)/2

        # total loss
        L_CrissCross = (L_async + L_sync + L_intra)/3

    return L_CrissCross

```

Table S1. Visual augmentation parameter details.

Augmentation	Parameters
Multi Scale Crop	min area = 0.08
Horizontal Flip	p = 0.5
	brightness = 0.4
	contrast = 0.4
Color Jitter	saturation = 0.4
	hue = 0.2
Gray Scale	p = 0.2
Gaussian Blur	p = 0.5
Cutout	max size = 20
	num = 1

Table S2. Visual augmentation summary.

	MSC	HF	CJ	GS	GB	C
Pretraining	✓	✓	✓	✓	✓	✓
Full-finetune	✓	✓	✓	✓	✗	✓
Linear evaluation	✓	✓	✓	✓	✗	✓

S2. Data Augmentation

Visual Augmentations. The parameters for visual augmentations are presented in Table S1. Some of the parameters are chosen from the literature, while the rest are found through empirical search. We set the parameters of Multi Scale Crop, Gaussian Blur, and Gray Scale as suggested in [11], and the parameters for Color Jitter are taken from [40]. We use TorchVision [43] for all the implementations of visual augmentations, except Cutout where we use the implementation available here¹. Please note that for the Cutout transformation, the mask is created with the mean value of the first frame in the sequence. We summarize the augmentation schemes used for pretraining and evaluation in Table S2.

Audio Augmentations. We present the parameters used for audio augmentations in Table S3. We use the Librosa [34] library to generate mel-spectrograms. We use the techniques proposed in [42] to perform Time Mask, Frequency Mask, and Time Warp transformations². The parameters for the audio augmentations are set empirically, except for Random Crop which we adopt from [41]. We summarize the augmentation scheme of pretraining and evaluation in Table S4.

S3. Datasets

Pretraining Datasets We use 3 datasets of different sizes for pretraining, namely, Kinetics-Sound [4], Kinetics400 [22], and AudioSet [16]. Kinetics-Sound is a small-scale action recognition dataset, which has a total of 22K video clips, distributed over 32 action classes. Kinetics400 is a medium-scale human action recognition dataset, originally collected from YouTube. It has a total of 240K training samples and 400 action classes. Please note that Kinetics-Sound is a

¹<https://github.com/uoguelph-mlrg/Cutout>

²<https://github.com/s3prl/s3prl>

Table S3. Audio augmentation parameter details.

Augmentation	Parameters
Volume Jitter	range = ± 0.2
Time Mask	max size = 20 num = 2
Frequency Mask	max size = 10 num = 2
Timewarp	wrap window = 20
Random Crop	range = [0.6, 1.5] crop scale = [1.0, 1.5]

Table S4. Audio augmentation summary.

	VJ	Mask	RC	TW
Pretraining	✓	✓	✓	✗
Linear evaluation	✓	✓	✓	✓

subset of Kinetics400, and consists of action classes which are prominently manifested audibly and visually [4]. Lastly, AudioSet [16] is a large-scale video dataset of audio events consisting of a total of 1.8M audio-video segments originally obtained from YouTube spread over 632 audio classes. Please note that none of the provided labels are used in self-supervised pretraining.

Downstream Datasets Following the standard practices of prior works [2, 3, 5, 26, 39, 40], we evaluate our self-supervised methods on two types of downstream tasks: (i) action recognition based on visual representations and (ii) sound classification based on audio representations. To perform action recognition, we use two popular benchmarks, i.e., UCF101 [57] and HMDB51 [27]. UCF101 consists of a total of 13K clips distributed among 101 action classes, while HMDB contains nearly 7K video clips distributed over 51 action categories. To perform sound classification, we use the popular benchmark ESC50 [46], which is a collection of 2K audio events comprised of 50 classes.

S4. Hyperparameters and Training Details

In this section, we present the details of the hyperparameters, computation requirements, as well as additional training details of self-supervised pretraining and full finetuning.

S4.1 Pretraining Details

We present the pretraining hyperparameters of CrissCross in Table S6. Most of the parameters remain the same across all 3 datasets, with the exception of a few hyperparameters such as learning rates and epoch size which are set depending on the size of the datasets. We train on Kinetics-Sound with a batch size of 512, on a single node with 4 Nvidia RTX-6000 GPUs. Next, when training on Kinetics-400 and AudioSet, we use 2 nodes and set the batch size to 2048. Adam [25] optimizer is used to train our proposed framework. We use

LARC³ [67] as a wrapper to the Adam optimizer to clip the gradients while pretraining with a batch size of 2048. In this work, we stick to batch sizes of 512 and 2048, because (i) as they show stable performance based on the findings of [12]; (ii) they fit well with our available GPU setups. Additionally, we perform mixed-precision training [35] using PyTorch AMP [43] to reduce the computation overhead.

Ablation Parameters. In the ablation study, we keep the training setup exactly identical across all the variants, with the exception of the learning rates, which we tune to find the best performance for that particular variant. For example, we set the base learning rate for visual-only and audio-only models as 0.0001 and 0.00001 respectively. Next, the predictor learning rates are set to 0.001 and 0.0001 for the visual-only and audio-only variants.

S4.2 Full Finetuning Details

The full finetuning hyperparameters for both the benchmarks are presented in Table S7. We use a batch size of 32 for the 32-frame input and 64 for the 8-frame input. We use an SGD optimizer with multi-step learning rate scheduler to finetune the video backbones. Please note that we perform the full finetuning on a single Nvidia RTX-6000 GPU.

S5. Downstream Evaluation Protocol

To evaluate the representations learned with self-supervised pretraining, we test the proposed framework in different setups, namely linear evaluation, full finetuning, and retrieval. The details of the evaluation protocols are mentioned below.

S5.1 Linear Evaluation

To perform linear evaluation of the learned representations on downstream tasks, we extract fixed features (also called frozen features) using the pretrained backbones. We train a linear classifier using a one-vs-all SVM on the fixed feature representations to compare different variants of our model. We present the details below.

Video. Following the protocols mentioned in [2, 48], we use 8-frame inputs to the video backbone, with a spatial resolution of 224². During training, we randomly pick 25 clips per sample to extract augmented representations, while during testing, we uniformly select 10 clips per sample. The augmentation techniques are mentioned in Section S2. We don't apply the Gaussian Blur while extracting the training features since it deteriorates the performance. Moreover, to perform a deterministic evaluation, we don't apply any augmentations during validation. The visual features are extracted from the final convolution layer and passed to a max-pool layer with a kernel size of (1, 4, 4) [40]. Finally,

³<https://github.com/NVIDIA/apex/blob/master/apex/parallel/LARC.py>

Table S5. Abbreviations and descriptions of the hyperparameters.

Abbreviations	Name	Description
bs	batch size	The size of a mini-batch.
es	epoch size	The total number of samples per epoch.
ep	total epochs	The total number of epochs.
lr	learning rate	
lr_{ab}	audio backbone lr	
lr_{vb}	video backbone lr	The learning rates to train the networks.
lr_{ap}	audio predictor lr	
lr_{vp}	video predictor lr	
lrs	learning rate scheduler	The learning rate scheduler to train the network.
ms	milestones	At every ms epoch the learning rate is decayed.
γ	lr decay rate	The learning rate is decayed by a factor of γ .
wd	weight decay	The weight decay used in the SGD optimizer.

Table S6. Pretext training parameters.

dataset	method	bs	es	ep	optim	lrs	lr_{vb} (start/end)	lr_{ab} (start/end)	lr_{vp}	lr_{ap}	wd	betas
Kinetics-Sound	CrissCross	512	220K	100	Adam	Cosine	0.0002/0	0.0002/0	0.002	0.002	0.0001	0.9, 0.999
Kinetics-400	CrissCross	2048	1M	100	Adam, LARC	Cosine	0.0002/0.0001	0.0002/0.0001	0.002	0.002	0.0001	0.9, 0.999
AudioSet	CrissCross	2048	3.5M	100	Adam, LARC	Cosine	0.0001/0	0.0001/0	0.001	0.001	0.0001	0.9, 0.999

Table S7. Full-finetuning hyperparameters for action recognition when pretrained on Kinetics-400.

dataset	input	es	bs	ep	ms	optim	lrs	lr	γ	wd	momentum	dropout
UCF101	8×224^2	95K	64	20	6/10/14	SGD	multi-step	0.0005	0.3	0.0	0.9	0.0
UCF101	32×224^2	95K	32	20	8/12/16	SGD	multi-step	0.00007	0.3	0.0	0.9	0.0
HMDB51	8×224^2	35K	64	20	6/10/14	SGD	multi-step	0.0005	0.1	0.0	0.9	0.0
HMDB51	32×224^2	35K	32	20	8/12/16	SGD	multi-step	0.0001	0.3	0.0	0.9	0.0

we use the learned visual representations to train a linear SVM classifier in order to perform action recognition.

Audio. In case of sound classification, we use 2 and 5-second audio inputs to extract audio representations. Following [44], we extract 10 epochs worth of augmented feature vectors from the training clips. During testing, when using 2-second inputs, we extract 10 equally spaced audio segments [3, 39, 40, 44], and when using 5-second inputs, we extract 1 segment [2, 48] from each sample. We perform the augmentations mentioned in Section S2 to extract the training features. We notice that unlike self-supervised pre-training, time warping improves the model performance in the linear evaluation. We do not apply any augmentations during validation. We extract the representations from the final convolution layer and pass it through a max-pool layer with a kernel size of (1, 3) and a stride of (1, 2) [44]. Similar to action recognition, we perform classification using a one-vs-all linear SVM classifier.

Please note that during training the SVM, we sweep the cost values between {0.00001, 0.00005, 0.0001, 0.0005, 0.001, 0.005, 0.01, 1} and report the best accuracy. In both the cases, action recognition and sound classification, we obtain the sample level prediction by averaging the clip level predictions and report the top-1 accuracy.

S5.2 Full Finetuning

Following earlier works [3, 5, 39, 40], we use the pretrained visual backbone along with a newly added fully-connected layer for full finetuning on UCF101 [57] and HMDB51 [27]. We adopt two setups for full finetuning, 8-frame inputs and 32-frame inputs. In both cases we use a spatial resolution of 224^2 . Lastly, we replace the final adaptive average-pooling layer with an adaptive max-pooling layer. We find that applying strong augmentations improves the model performance in full-finetuning. Please see the augmentation details in Section S2. During testing, we extract 10 equally spaced clips from each sample and do not apply any augmentations. We report the top-1 accuracy at sample level prediction by averaging the clip level predictions. We use an SGD optimizer with a multi-step learning rate scheduler to finetune the model. We present the hyperparameters of full-finetuning in Table S7.

S5.3 Retrieval

In addition to full-finetuning, we also perform retrieval to test the quality of the representations in an unsupervised setup. We follow the evaluation protocol laid out in [44, 66]. We uniformly select 10 clips per sample from both training

Table S8. Architecture of the video backbone: R(2+1)D-18.

Layer	X_s	X_t	C	K_s	K_t	S_s	S_t
frames	112	8	3	-	-	-	-
conv1	56	8	64	7	3	2	1
maxpool	28	8	64	3	1	2	1
block2.1.1	28	8	64	3	3	1	1
block2.1.2	28	8	64	3	3	1	1
block2.2.1	28	8	64	3	3	1	1
block2.2.2	28	8	64	3	3	1	1
block3.1.1	14	4	128	3	3	2	2
block3.1.2	14	4	128	3	3	1	1
block3.2.1	14	4	128	3	3	1	1
block3.2.2	14	4	128	3	3	1	1
block4.1.1	7	2	256	3	3	2	2
block4.1.2	7	2	256	3	3	1	1
block4.2.1	7	2	256	3	3	1	1
block4.2.2	7	2	256	3	3	1	1
block5.1.1	4	1	512	3	3	2	2
block5.1.2	4	1	512	3	3	1	1
block5.2.1	4	1	512	3	3	1	1
block5.2.2	4	1	512	3	3	1	1
avg-pool	-	-	512	-	-	-	-

and test splits. We fit 2-second inputs to the backbone to extract representations. We empirically test additional steps such as l2-normalization and applying batch-normalization on the extracted features, and notice that they do not help the performance. Hence, we simply average the features extracted from the test split to query the features of the training split. We compute the cosine distance between the feature vectors of the test clips (query) and the representations of all the training clips (neighbors). We consider a correct prediction if k neighboring clips of a query clip belong to the same class. We calculate accuracies for $k = 1, 5, 20$. We use the NearestNeighbors⁴ API provided in SciKit-Learn in this experiment.

S6. Architecture Details

In this study we use a slightly modified version of R(2+1)D-18 [60] as the video backbone as proposed in [40], and ResNet-18 [20] as the audio backbone. For the sake of completeness we present the architecture details in Table S8 and Table S9, respectively. The predictor and projector heads are made of fully-connected layers following [12], and their architecture details are presented in Table S10.

S7. Additional Results

S7.1 Effect of the Size of Pretraining Datasets

We use 3 different sized datasets, i.e., Kinetics-Sound, Kinetics-400, and AudioSet. In Table S11, we present the results of CrissCross trained on all of the 3 datasets. We notice a steady improvement in performance as the dataset size increases. The results presented in Table S11 are obtained by linear evaluation on split-1 of UCF101 and ESC50.

⁴sklearn.neighbors.NearestNeighbors

Table S9. Architecture of the audio backbone: ResNet-18.

Layer	X_f	X_t	C	K_s	K_t	S_f	S_t
spectrogram	80	100	1	-	-	-	-
conv1	40	50	64	7	7	2	2
maxpool	20	25	64	3	3	2	2
block2.1.1	20	25	64	3	3	2	2
block2.1.2	20	25	64	3	3	2	2
block2.2.1	20	25	64	3	3	2	2
block2.2.2	20	25	64	3	3	2	2
block3.1.1	10	13	128	3	3	2	2
block3.1.2	10	13	128	3	3	2	2
block3.2.1	10	13	128	3	3	2	2
block3.2.2	10	13	128	3	3	2	2
block4.1.1	5	7	256	3	3	2	2
block4.1.2	5	7	256	3	3	2	2
block4.2.1	5	7	256	3	3	2	2
block4.2.2	5	7	256	3	3	2	2
block5.1.1	3	4	512	3	3	2	2
block5.1.2	3	4	512	3	3	2	2
block5.2.1	3	4	512	3	3	2	2
block5.2.2	3	4	512	3	3	2	2
avg-pool	-	-	512	-	-	-	-

Table S10. Architecture of projector and predictor heads.

Head	Layer	Dimensions
Projector	input	512
	fc-bn-relu	2048
	fc-bn-relu	2048
Predictor	fc-bn	2048
	input	2048
	fc-bn-relu	512
	fc	2048

Table S11. The effect of the size of pretraining dataset.

Pretraining Dataset	Size	UCF101	ESC50
Kinetics-Sound	22K	74.8	79.0
Kinetics-400	240K	79.9	82.0
AudioSet	1.8M	83.7	84.0

Table S12. **Ablation study.** In this ablation study we pretrain the variants on Kinetics-400 and perform linear evaluation on fixed feature representations obtained from split-1 of UCF101 and ESC50 to perform action recognition and sound classification respectively.

Method	UCF101	ESC50
$\mathcal{L}_{sync} + \mathcal{L}_{intra}$	75.8	78.5
$\mathcal{L}_{async} + \mathcal{L}_{intra}$	74.9	76.3
$\mathcal{L}_{CrissCross}$	79.9	82.0

S7.2 Ablation Study on Kinetics-400

Here we present an ablation study using Kinetics-400 [22], comparing the performance of CrissCross to its multi-modal ablation competitors, as demonstrated in Table 1. We observe that CrissCross significantly outperforms its multi-modal ablation variants, indicating the importance of op-

Table S13. **State-of-the-art comparison on sound classification.** We present the Top-1 accuracy averaged over all the splits on ESC50 using different pretraining datasets. Additionally, we present the architecture details and finetuning input size of the respective methods. The following abbreviations are used in the table, FS: Flickr-SoundNet, KS: Kinetis-Sound, K400: Kinetics-400, AS: AudioSet.

Method	Backbone	Pretraining Dataset	Finetune Input Size	ESC50
Human Performance [4]	-	-	-	81.3
RandomForest [46]	MLP	-	-	44.3
ConvNet [45]	ConvNet-4	-	-	64.5
ConvRBM [51]	ConvNet-4	-	-	86.5
SoundNet [6]	ConvNet-8	FS	1 Sec.	74.2
L3 [4]	ConvNet-8	FS	1 Sec.	79.3
	VGG-8	FS	2 Sec.	82.3
AVTS [26]	VGG-8	K400	2 Sec.	76.7
	VGG-8	AS	2 Sec.	80.6
XDC [3]	ResNet-18	K400	2 Sec.	78.0
	ResNet-18	AS	2 Sec.	84.8
AVID [40]	ConvNet-9	K400	2 Sec.	79.1
	ConvNet-9	AS	2 Sec.	89.1
GDT [44]	ResNet-9	AS	2 Sec.	88.5
MMV [2]	ResNet-50	AS	5 Sec.	85.6
BRAVE [48]	ResNet-50	AS	5 Sec.	90.4
CrissCross	ResNet-18	KS	2 Sec.	79.5
	ResNet-18	KS	5 Sec.	82.8
	ResNet-18	K400	2 Sec.	81.5
	ResNet-18	K400	5 Sec.	86.8
	ResNet-18	AS	2 Sec.	86.7
	ResNet-18	AS	5 Sec.	90.5

timizing both synchronous and asynchronous cross-modal losses. The results are presented in Table S12.

S7.3 Extended List of Prior Works

An extended list of prior works on sound classification and action recognition are presented in Table S13 and S14, respectively.

S7.4 Training Statistics

To provide a better understanding of our training process, we present the loss curves of self-supervised pretraining on Kinetics-400 in Figure S1. We notice that the intra-modal losses reach a steady state quite early, compared to the cross-modal losses. The total loss still decreases beyond our scheduled training iterations. However, we stop the training when no improvement is noticed in the downstream tasks.

S7.5 Qualitative Analyses

To perform a qualitative analysis of the learned representations, we visualize the nearest neighborhoods of video-to-video and audio-to-audio retrieval. In this experiment, we use Kinetics-400 [22] to pretrain CrissCross. The pre-trained backbones are then used to extract training and validation feature vectors from Kinetics-Sound [4]. We use the Kinetics-Sound for retrieval experiment as it consists of action classes which are prominently manifested both audibly and visually. Next, we use the features extracted from the validation split to query the training features. We present the qualitative results in Figure S2 and S3.

Table S14. **State-of-the-art comparison on action recognition.** We present the Top-1 accuracy averaged over all the splits on UCF101 and HMDB51 using different pretraining datasets. Additionally, we present the architecture details and finetuning input size of the respective methods. The following abbreviations are used in the table, KS: Kinetis-Sound, K400: Kinetics-400, K700: Kinetics-700, AS: AudioSet.

Method	Backbone	Pretraining Dataset	Finetune Input Size	UCF101	HMDB51
Scratch [3]	R(2+1)D-18	-	32×224 ²	54.5	24.1
Fully Supervised [32]	3D-ResNet18	KS	32×224 ²	86.9	53.1
Fully Supervised [3]	R(2+1)D-18	K400	32×224 ²	94.2	65.1
Fully Supervised [44]	R(2+1)D-18	K400	32×224 ²	95.0	74.0
ClipOrder [66]	R(2+1)D-18	K400	16×112 ²	72.4	30.9
MotionPred [65]	C3D	K400	16×112 ²	61.2	33.4
DPC [18]	S3D	K400	25×128 ²	75.7	35.7
RotNet3D [21]	3D-ResNet18	K400	16×112 ²	62.9	33.7
ST-Puzzle [24]	3D-ResNet18	K400	16×80 ²	65.8	33.7
SpeedNet [8]	S3D	K400	16×224 ²	81.1	48.8
CBT [58]	S3D	K400	16×112 ²	79.5	44.6
AVTS [26]	MC3-18	K400	25×224 ²	84.1	52.5
	MC3-18	AS	25×224 ²	87.7	57.3
SeLaVi [5]	R(2+1)D-18	K400	32×112 ²	83.1	47.1
	R(2+1)D-18	K400	8×224 ²	74.2	39.0
XDC [3]	R(2+1)D-18	K400	32×224 ²	86.8	52.6
	R(2+1)D-18	AS	8×224 ²	84.9	48.8
	R(2+1)D-18	AS	32×224 ²	91.2	61.0
	R(2+1)D-18	K400	8×224 ²	83.7	49.5
AVID [40]	R(2+1)D-18	K400	32×224 ²	87.5	60.8
	R(2+1)D-18	AS	8×224 ²	88.6	57.6
	R(2+1)D-18	AS	32×224 ²	91.5	64.7
GDT [44]	R(2+1)D-18	K400	32×224 ²	89.3	60.0
	R(2+1)D-18	AS	32×224 ²	92.5	66.1
Robust-xID [39]	R(2+1)D-18	K400	8×224 ²	81.9	49.5
	R(2+1)D-18	K400	32×224 ²	85.6	55.0
MMV [2]	R(2+1)D-18	K400	32×224 ²	91.5	70.1
BraVe [48]	R(2+1)D-18	AS	32×224 ²	94.1	71.1
	3D-ResNet18	KS	32×224 ²	77.2	40.6
	3D-ResNet18	K700(240K)	32×224 ²	90.2	61.8
CM-ACC [32]	3D-ResNet18	AS(240K)	32×224 ²	90.7	62.3
	3D-ResNet18	AS	32×224 ²	94.1	66.8
	R(2+1)D-18	AS	32×224 ²	93.5	67.2
CrissCross	R(2+1)D-18	KS	8×224 ²	84.0	51.2
	R(2+1)D-18	KS	32×224 ²	88.3	60.5
	R(2+1)D-18	K400	8×224 ²	86.9	54.3
	R(2+1)D-18	K400	32×224 ²	91.5	64.7
	R(2+1)D-18	AS	8×224 ²	89.4	58.3
	R(2+1)D-18	AS	32×224 ²	92.4	66.8

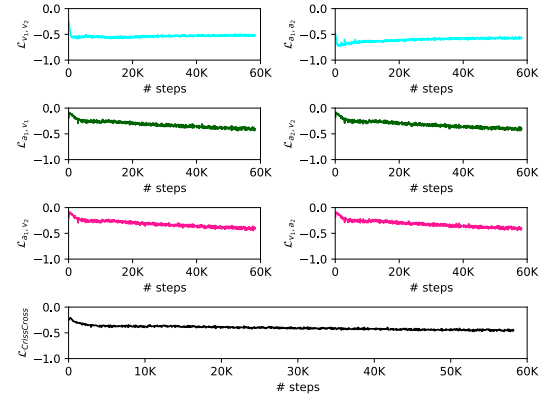


Figure S1. **CrissCross training curves.** We present the loss curves when pretraining on Kinetics-400. \mathcal{L}_{v_1, v_2} and \mathcal{L}_{a_1, a_2} refer to intra-modal losses; \mathcal{L}_{a_1, v_1} and \mathcal{L}_{a_2, v_2} denote synchronous cross-modal losses; and finally \mathcal{L}_{a_1, v_2} and \mathcal{L}_{v_1, a_2} refer to asynchronous cross-modal losses. Note that the minimum possible value for each loss is -1 .



Figure S2. Visualization of video-to-video retrieval. The frames with **black** borders represent the query embedding, and the next 5 frames represent the top-5 neighborhoods. We highlight the correct retrievals with **green**, while the wrong ones are marked with **red**. Additionally, we also mention the class names at the bottom of each frame. We notice very few instances of wrong retrieval, which generally occur when the visual scenes are highly similar, for instance ‘playing piano’ and ‘playing organ’, ‘playing saxophone’ and ‘playing clarinet’.



Figure S3. **Visualization of audio-to-audio retrieval.** The frames with **black** borders represent the query embedding, and the next 5 frames represent the top-5 neighborhoods. We highlight the correct retrievals with **green**, while the wrong ones are marked with **red**. Additionally, we also mention the class names at the bottom of each frame. We notice very few instances of wrong retrieval, which generally occur when the sound events are audibly very similar for instance, ‘playing keyboard’ and ‘playing xylophone’, ‘playing saxophone’ and ‘playing accordion’.